

Lawrence Berkeley National Laboratory

Recent Work

Title

FAR INFRARED OPTICAL PROPERTIES OF NbSe₃

Permalink

<https://escholarship.org/uc/item/9qc7t33d>

Authors

Challener, W.A.

Richards, P.L.

Publication Date

1984-06-01

c2



Lawrence Berkeley Laboratory

UNIVERSITY OF CALIFORNIA

RECEIVED
BERKELEY, CALIF. 94720

Materials & Molecular Research Division

AUG 20 1984

LIBRARY AND
DOCUMENTS SECTION

Submitted to Solid State Communications

FAR INFRARED OPTICAL PROPERTIES OF NbSe₃

W.A. Challener and P.L. Richards

June 1984

TWO-WEEK LOAN COPY
*This is a Library Circulating Copy
which may be borrowed for two weeks.*



LBL-16855 Rev.
c2

DISCLAIMER

This document was prepared as an account of work sponsored by the United States Government. While this document is believed to contain correct information, neither the United States Government nor any agency thereof, nor the Regents of the University of California, nor any of their employees, makes any warranty, express or implied, or assumes any legal responsibility for the accuracy, completeness, or usefulness of any information, apparatus, product, or process disclosed, or represents that its use would not infringe privately owned rights. Reference herein to any specific commercial product, process, or service by its trade name, trademark, manufacturer, or otherwise, does not necessarily constitute or imply its endorsement, recommendation, or favoring by the United States Government or any agency thereof, or the Regents of the University of California. The views and opinions of authors expressed herein do not necessarily state or reflect those of the United States Government or any agency thereof or the Regents of the University of California.

FAR INFRARED OPTICAL PROPERTIES OF NbSe₃

W. A. Challener* and P. L. Richards

Department of Physics, University of California and
Materials and Molecular Research Division, Lawrence Berkeley Laboratory,
Berkeley, California 94720, U.S.A.

(Received 1984 by H. Suhl)

We have measured the far infrared reflectance of NbSe₃, and used models of the frequency dependent conductivity to fit the data. General arguments show that at 2 K a charge density wave (CDW) energy gap exists between 120 and 190 cm⁻¹, the relaxation time(s) of the free carriers and CDW pinned mode is $>3 \times 10^{-12}$ s, and the ratio of the free carrier concentration to band mass is $<2 \times 10^{20}$ cm⁻³/m₀.

Introduction

NbSe_3 is a prototype for sliding charge density wave (CDW) systems. It undergoes independent and incommensurate CDW phase transitions at $T_1 = 145$ K, and $T_2 = 59$ K. At each transition a fraction of the free carriers present at room temperature condense into a CDW. The oscillator strength of the condensed carriers can appear in a low frequency pinned mode,¹ a single-particle continuum above a CDW energy gap,² and coupled CDW carrier-optical phonon modes (phase phonons).³ We have used a Kramers-Kronig analysis to obtain an estimate of the frequency dependence of the conductivity, $\sigma(\omega)$, from our measured far infrared (FIR) reflectance of NbSe_3 . The qualitative features of the conductivity include many phonons which appear below T_2 , a CDW energy gap, and a low frequency contribution from the free carriers and the pinned mode.

A detailed model fit to the conductivity reproduces the data very accurately. It gives estimates of carrier concentrations and relaxation times, electron-phonon coupling constants and the size of the CDW energy gap. When analyzing a limited data set from a very complicated physical system like NbSe_3 , however, one cannot be entirely certain that all of the relevant physics is included in the model. As our knowledge about NbSe_3 increases, the fitting procedures used here may have to be modified. It seems clear, however, that the far infrared reflectance data will provide strong constraints to any proposed model.

Sample Preparation and Apparatus

Our NbSe_3 fibers were supplied by P. Monceau and have typical widths of 5 μm and lengths of 5 mm, with a residual resistivity ratio ($\rho_{300\text{K}} / \rho_{4.2\text{K}}$) of ~ 20 . Reflectance samples were made by sticking fibers on mylar tape approximately parallel to each other, and packed closely enough compared to FIR wavelengths that the sample was opaque to FIR radiation polarized parallel to the fibers. Except for a few thin spots, the sample was essentially opaque to visible light. For FIR radiation polarized parallel to the fibers, the sample approximates a single-crystal surface, although surface roughness scatters light from the beam and makes accurate normalization of the reflectance difficult. Our approach requires that the IR wavelength must be large compared

with the characteristic surface roughness, and so limits the frequency range over which data can be interpreted. As an approximate correction for surface scattering effects, the data were normalized to the reflectance of the sample after it was covered with evaporated gold. Measurements of the reflectance for radiation polarized perpendicular to the fibers are not included because they are thought to be dominated by the parallel reflectance of misaligned fibers.

Data and Analysis

At room temperature the FIR reflectance of NbSe_3 is large (>90%) and featureless. Below T_2 a reflectance edge begins to develop at 140 cm^{-1} , which becomes quite sharp by 2 K as is shown in Fig. 1. Approximately forty phonon lines appear in the reflectance below T_2 , and by 2 K about 22 of these lines are very strong. At frequencies below 100 cm^{-1} the lines are sharp dips with linewidths of $\sim 1 \text{ cm}^{-1}$. Above 140 cm^{-1} the lines appear as sharp peaks and above $\sim 200 \text{ cm}^{-1}$ there is a noticeable broadening of the phonon linewidths. Many of the lines appear to be doublets.

The optical constants for NbSe_3 at 2 K were obtained by a Kramers-Kronig analysis of the reflectance using standard extrapolation procedures.⁴ The real part of the dielectric function is strongly negative below 100 cm^{-1} . Above 300 cm^{-1} it remains fairly constant and close to zero. Between 140 cm^{-1} and 250 cm^{-1} there are several zero crossings which arise from phonon dispersions. The real part of the conductivity, $\sigma_1(\omega)$, is shown in Fig. 2(a). The finite frequency range and uncertain normalization of the data make the conductivity scale uncertain by a factor of order four, but the important spectral features in the optical constants at 2 K have been obtained from a variety of approaches to both the measurement and the analysis.

Standard models for the frequency dependence of the conductivity for free and condensed carriers were used to fit our estimate of the conductivity. A Drude function, with $\sigma(\omega) = \sigma_{\text{dc}}(1+i\omega\tau)^{-1}$, was used to model the oscillator strength of the free carriers. The oscillator strength of the condensed carriers was modeled according to the theories of Lee, Rice, and Anderson² (LRA) and M. J. Rice,³ using Eqs. 2-8 of Ref. 3, with $V = 0$, as is appropriate for NbSe_3 . The oscillator strength

of the pinned mode was included in this model by treating it as a low frequency phonon mode. Thirty-four phase phonon modes were included with frequencies and coupling constants as adjustable parameters. The excellent fit to $\sigma_1(\omega)$ shown in Fig. 2(b) has been obtained using the parameters in Table I. We now discuss important aspects of these results.

Phase Phonons

In good conductors like NbSe_3 , phonons are generally unobservable in the FIR because of screening by the free carriers. In the distorted lattice, the optical phonons with a $2 k_F$ wavevector are folded to the center of the Brillouin zone. These new zone center phonons may form coupled modes with the CDW carriers called phase phonons³ if they satisfy symmetry requirements. In NbSe_3 , only the 24 totally symmetric (A_g) modes of the undistorted lattice have the correct symmetry for first-order coupling to the condensed carriers. The number of the strong phonons we see in the FIR spectrum of NbSe_3 is in good agreement with this number of A_g modes. The many weaker phonons in the FIR spectrum may be due to coupling to $4 k_F$ optical phonons, or to phonons which acquire A_g symmetry only in the distorted lattice. Because these phonons begin to appear in the FIR spectrum only below T_2 , we believe that these are phase phonons coupled to the T_2 CDW. It is not clear why phase phonons coupled to the T_1 CDW do not appear in the FIR spectrum below T_1 .

When the frequencies of phase phonons occur below the CDW energy gap, they appear as peaks in σ_1 with their bare phonon linewidth. Phase phonons with frequencies above the energy gap, however, can decay through creation of electron hole pairs, and have their linewidths considerably broadened. Such modes give rise to Fano-like interference dips in the conductivity of the single-particle continuum.⁵ It can be seen from Fig. 2 that the phonons above $\sim 200 \text{ cm}^{-1}$ give rise to this interference effect in the conductivity of NbSe_3 . The measured conductivity of the phase phonons can be used³ to obtain estimates of the electron-phonon coupling constants.

CDW Energy Gap

The Fano interference effect is strong evidence for a CDW energy gap below $\sim 190 \text{ cm}^{-1}$. In addition, there is a general rise in $\sigma_1(\omega)$

above $\sim 120 \text{ cm}^{-1}$, and by $\sim 200 \text{ cm}^{-1}$ it is clear that this rise is not due solely to the phonon modes. We interpret this additional contribution to the conductivity as a single-particle continuum above an energy gap. It could not arise from an underestimate of the diffuse scattering from the sample, which would have the effect of monotonically decreasing $\sigma_1(\omega)$ in this region. We conclude that there is a CDW energy gap with $120 \lesssim 2\Delta \lesssim 190 \text{ cm}^{-1}$. The value of 190 cm^{-1} was used for the detailed fit shown in Fig. 2. These results should be compared with the mean field value⁶ $2\Delta = 3.5 k_B T_C = 140 \text{ cm}^{-1}$ for the T_2 CDW.

Pinned Mode and Free Carriers

Below 100 cm^{-1} , $\sigma_1(\omega)$ falls with increasing frequency. We believe this fall is the tail of the contribution to the conductivity from both the CDW pinned mode and the free carriers. Several alternative arguments can be used to obtain the relaxation time and oscillator strength of free carriers and pinned mode. If we assume that the conductivity measured at microwave frequencies relaxes as $(\omega\tau)^{-2}$ in the FIR, and that the dc conductivity of our NbSe_3 fibers at 2 K is $\sim 10^5 (\Omega \text{ cm})^{-1}$, then the FIR reflectance minimum of less than 40% at 140 cm^{-1} requires a relaxation time at 2 K of $> 3 \times 10^{-12} \text{ s}$. From this result, we can estimate the combined oscillator strength of the pinned mode and the free carriers. It is convenient to express the oscillator strength in terms of the ratio of the carrier concentration to the band mass. From the equation $n/m^* \approx \sigma_{dc}/(\tau e^2)$, we get $n/m^* < 2 \times 10^{20} \text{ cm}^{-3}/m_0$, where m_0 is the free electron mass.

An alternative, and perhaps better, method for estimating the total low frequency oscillator strength is to integrate the area under the curve of $\sigma_1(\omega)$. Taking into account the uncertainties of the reflectance normalization, the Kramers-Kronig analysis of the data indicates a relaxation time of $> 10^{-11} \text{ s}$ and $n/m^* < 5 \times 10^{19} \text{ cm}^{-3}/m_0$ for the combined pinned mode and free carriers.

The detailed fit shown in Fig. 2 gives a relaxation time for this low frequency mode of $4.4 \times 10^{-13} \text{ s}$. This number is outside the limits set by the previous two estimates. This estimate of the relaxation time from the fit to the conductivity, however, is especially sensitive to errors in the normalization of the reflectance at low frequencies. Oscillator

strengths of $n/m^* = 2.8 \times 10^{17} \text{ cm}^{-3}/m_0$ for the pinned modes and 1.2×10^{18} for the free carriers, giving a total of $1.5 \times 10^{18} \text{ cm}^{-3}/m_0$, were used in the detailed fit. Errors in the normalization of the reflectance could make this number too small by about a factor of five. A background dielectric constant of 1.4 is used in the fit.

These parameter values are compared to other estimates of the carrier concentration from the literature in Table II. A two-band model⁷ of magnetotransport data for NbSe₃ gives a total concentration of free carriers which remain uncondensed at temperatures well below T_2 of $7 \times 10^{18} \text{ cm}^{-3}$. This is consistent with our FIR data. However, similar estimates based upon the analysis of narrow band noise measurements,^{8,9} assuming that the relevant periodicity is the CDW wavelength and that there are $\geq 10^{21} \text{ cm}^{-3}$ carriers at room temperature, yield concentrations $\geq 5 \times 10^{20} \text{ cm}^{-3}$. Unless one is willing to accept band masses $> 10 m_0$, the FIR data are inconsistent with the estimates based on the noise measurements. This disagreement suggests that the relevant periodicity in the analysis of the narrow band noise may not be the CDW wavelength as is generally, but not universally,¹⁰⁻¹³ assumed.

Pinned Mode and Single-Particle Continuum

In the CDW state, the $2k_F$ acoustic phonons form a collective mode with the CDW carriers, which is often called a phason. The phason corresponds to phase oscillations of the CDW at the pinning frequency and contributes to the ac conductivity. According to the LRA theory,² the fraction of the oscillator strength of the condensed carriers which appears in the phason is determined by the ratio, m^*/M_F , of the carrier band mass to the effective mass per condensed carrier of the CDW. Although not explicitly discussed, a simple classical harmonic oscillator model⁹ of CDW transport gives a similar result. By contrast, the tunneling model¹ of CDW transport attributes most of the ac conductivity of the pinned CDW to photon assisted tunneling.

One feature of the theory plays an important role in fitting our data. As $m_F/m^* \rightarrow \infty$ in the LRA theory, a sharp peak develops in σ_1 at the energy gap. If the effective mass ratio m_F/m^* is sufficiently small, the sharp peak in σ_1 does not occur. This peak is a consequence of their assumption of a strictly one-dimensional band structure.

For a material like NbSe₃, however, the Fermi surface has higher effective dimensionality, so the peak in σ_1 at the energy gap should be considerably rounded even when $m_F/m^* \rightarrow \infty$.

To produce the fit to the conductivity shown in Fig. 2(b), we have used the equations of LRA² and of Rice.³ The CDW energy gap has been chosen at 190 cm⁻¹. It is necessary to put a large fraction (in this case 20%) of the oscillator strength of the condensed carriers in the pinned mode to avoid the sharp peak in the theoretical σ_1 curve at the energy gap, which is not observed. Fitting the data with an energy gap at lower frequencies degrades the fit and requires that an even larger fraction of the oscillator strength of the condensed carriers appear in the pinned mode. If the oscillator strength in the pinned mode appears in the phason as suggested by the classical model of CDW transport,⁹ then we obtain a CDW effective mass, $M_F < 5 m^*$, from the LRA theory.² This is much smaller than is generally assumed and may indicate the inappropriateness of using the one-dimensional LRA theory to model the conductivity of NbSe₃.

The ratio n/m^* of the total condensed carrier concentration to band mass from the fit is 1.4×10^{19} cm⁻³/m₀. Errors in the normalization of the data could make this value too small by about a factor of 5. The two-band model⁷ of magnetotransport data estimates the CDW carrier concentration for the T₂ CDW to be 2×10^{19} cm⁻³, while estimates from analysis of narrow band noise measurements^{8,9} of the concentration of carriers condensed in the T₂ CDW range from 0.62×10^{20} cm⁻³ to 1.5×10^{21} cm⁻³. The small ratio of carrier concentration to band mass from the fit to the FIR data may indicate either that there are very large carrier band masses, or that a substantial amount of the oscillator strength of the T₂ CDW carriers occurs at frequencies above 350 cm⁻¹ and is not being included in our extrapolation of the available data. Our ability to estimate the high frequency oscillator strength is limited by both the frequency range of the data and the one-dimensional approximation used in the theory.

Conclusions

Many optical phonons are found to become IR-active through coupling to the T_2 CDW. Fitting the conductivity obtained from a Kramers-Kronig analysis of our reflectance data leads to an estimated width of the CDW energy gap between 120 and 190 cm^{-1} . Phonons above the energy gap appear as Fano antiresonances, as has been seen in organic CDW systems. Our FIR measurements indicate that the ratio of the free carrier concentration to the band mass at 2 K is $\ll 2 \times 10^{20} \text{ cm}^{-3}/m_0$.

Acknowledgments

We particularly like to thank P. Monceau, who provided the NbSe₃, used for these measurements, and L.M. Falicov, P.A. Lee, N.P. Ong, A.M. Portis, and T. Rasing for useful discussions. This work was supported by the Director, Office of Energy Research, Office of Basic Energy Sciences, Materials Sciences Division of the U.S. Department of Energy under Contract No. DE-AC03-76SF00098.

References

- * Present address: Los Alamos National Laboratory, Physics Department, Section P-10, Los Alamos, New Mexico 87545, U.S.A.
- ¹J. Bardeen, Proceedings of the International School of Physics "Enrico Fermi," Varenna, Italy, July 4-6, 1983 (to be published); G. Grüner, A. Zettl, W.G. Clark, J. Bardeen, Phys. Rev. B24, 7247 (1981).
- ²P.A. Lee, T.M. Rice, P.W. Anderson, Sol. St. Commun. 14, 703 (1974).
- ³M.J. Rice, Phys. Rev. Lett. 37, 36 (1976).
- ⁴F. Wooten, Optical Properties of Solids, Academic Press, New York (1972), p. 248.
- ⁵M.J. Rice, L. Pietronero, P. Brüesch, Sol. St. Commun. 21, 757 (1977).
- ⁶H. Fröhlich, Proceedings of the Royal Society London A223, 296 (1954); C.G. Kuper, Proc. Roy. Soc. London A227, 214 (1955).
- ⁷N.P. Ong, Phys. Rev. B18, 5272 (1978).
- ⁸J. Richard, P. Monceau, M. Renard, Phys. Rev. B25, 948 (1982).
- ⁹G. Grüner, A. Zawadowski, P.M. Chaikin, Phys. Rev. Lett. 46, 511 (1981).
- ¹⁰N.P. Ong, C.M. Gould, Sol. St. Commun. 37, 25 (1980).
- ¹¹P. Bak, Phys. Rev. Lett. 48, 692 (1982).
- ¹²M. Weger, B. Horovitz, Sol. St. Commun. 43, 583 (1982).
- ¹³P. Monceau, M. Renard, J. Richard, M.C. Saint-Lager, H. Salva, Z.Z. Wang, preprint.

TABLE I

PHASE PHONON PARAMETERS USED FOR CONDUCTIVITY FIT IN FIGURE 2(b)

phonon freq., ν_n	coupling constant, λ_n	line- width, ν_{rn}	phonon freq., ν_n	coupling constant, λ_n	line- width, ν_{rn}
40 cm^{-1}	.25	1 cm^{-1}	162 cm^{-1}	.0056	2 cm^{-1}
48	.057	1	166	.008	2
52	.057	1	170	.02	2
67	.044	1	175	.004	2
71	.141	1	179	.0117	2
76	.036	1	185	.019	2
81	.014	1	188	.006	1
93	.0216	1	197	.01	2
99	.032	1	207	.005	2
108	.0046	1	211	.0075	2
111	.0046	1	221	.0005	2
120	.001	1	227	.0005	2
143	.0075	1	232	.001	2
151	.0014	2	241	.0065	2
154	.002	2	251	.001	2
155	.0027	2	256	.005	2
158	.01	2	265	.001	2

TABLE II

ESTIMATES OF OSCILLATOR STRENGTHS, RELAXATION TIMES, AND CARRIER CONCENTRATIONS DISCUSSED IN THE TEXT

basis of estimate	combined oscillator strength of pinned mode and free carriers at 2 K (cm^{-3}/m_0)	relaxation time at 2 K (s)
reflectance at 140 cm^{-1}	$< 2 \times 10^{20}$	$> 3 \times 10^{-12}$
sum rule	$< 5 \times 10^{19}$	$> 10^{-11}$
fit to the conductivity	1.5×10^{18}	4.4×10^{-13}

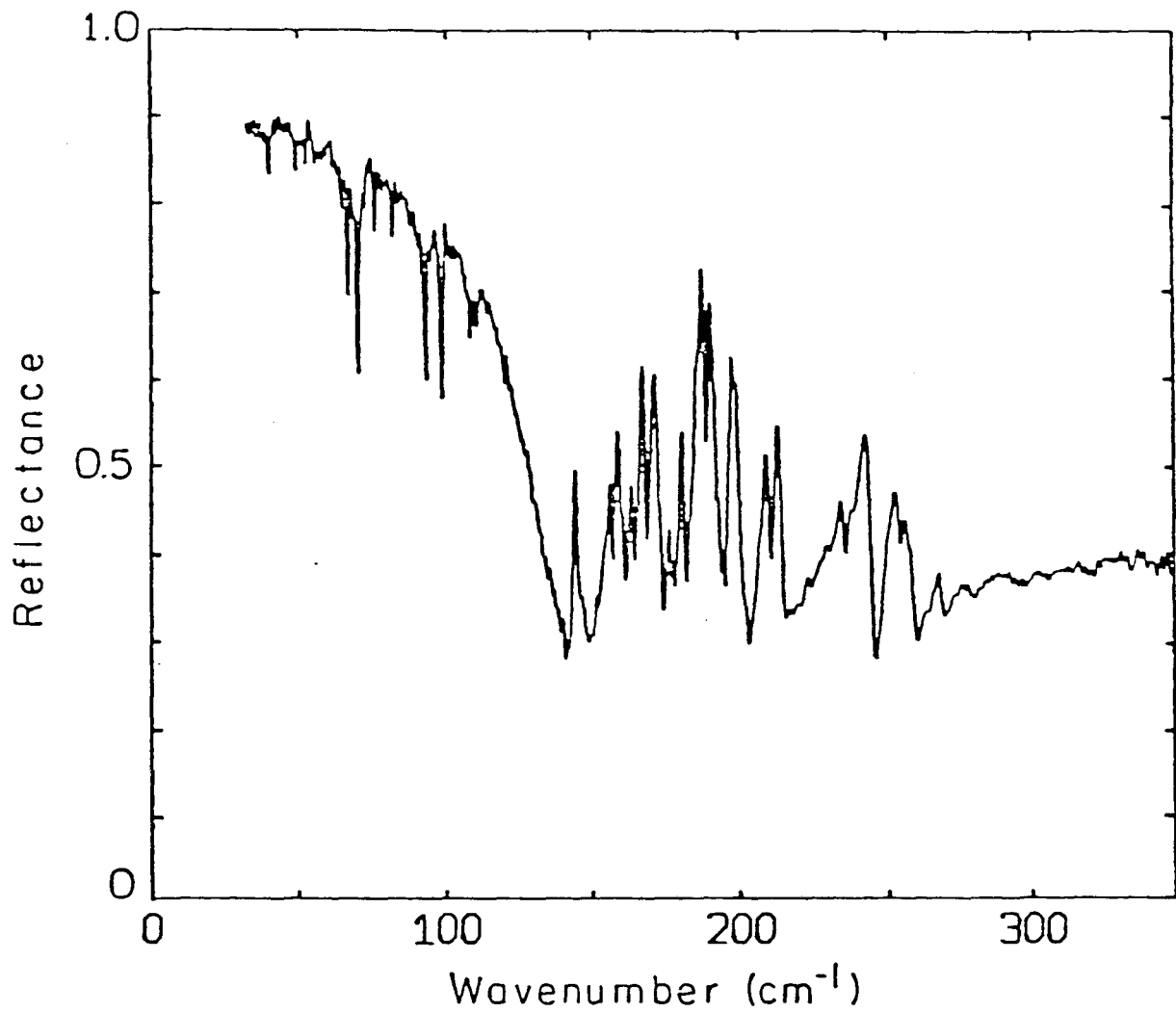
basis of estimate	concentration of free carriers at 2 K (cm^{-3})	concentration of carriers condensed in T_2 CDW at 2 K (cm^{-3})
two-band model of magnetotransport ⁷	7×10^{18}	2×10^{19}
narrow band noise ⁸	$\sim 10^{21}$	$1 - 1.5 \times 10^{21}$
narrow band noise ⁹	$\geq 5 \times 10^{20}$	$0.62 - 1.96 \times 10^{20}$

Figure Captions

Figure 1. Reflectance of NbSe₃ at 2 K for light polarized parallel to the fiber axis.

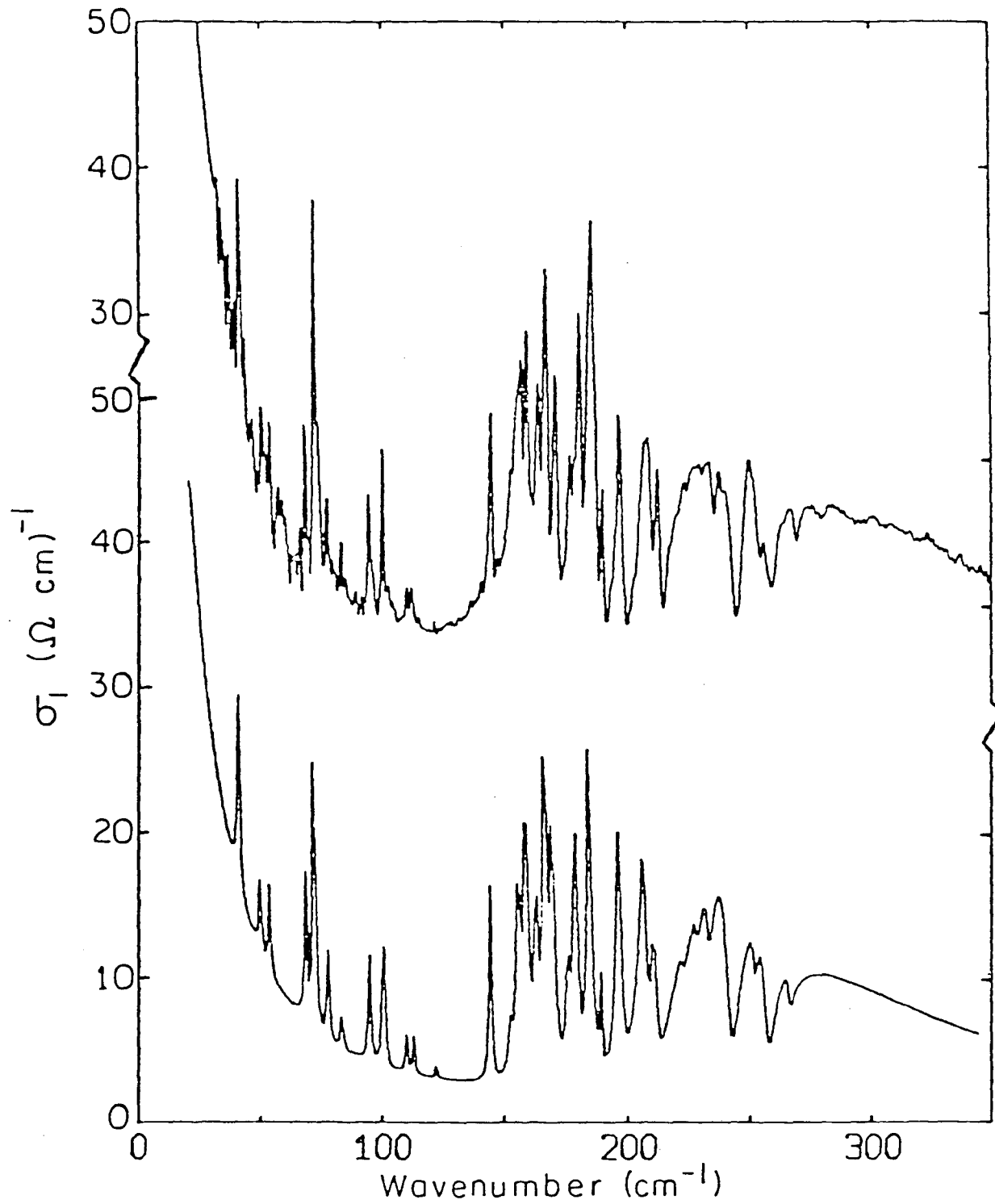
Figure 2. (a) Kramers-Kronig calculation of σ_1 from the measured reflectance in Fig. 1.

(b) Fit to σ_1 using equations described in the text and parameters in Tables I and II.



XBL 839-6270

Figure 1



XBL 839-6269

Figure 2

This report was done with support from the Department of Energy. Any conclusions or opinions expressed in this report represent solely those of the author(s) and not necessarily those of The Regents of the University of California, the Lawrence Berkeley Laboratory or the Department of Energy.

Reference to a company or product name does not imply approval or recommendation of the product by the University of California or the U.S. Department of Energy to the exclusion of others that may be suitable.

TECHNICAL INFORMATION DEPARTMENT
LAWRENCE BERKELEY LABORATORY
UNIVERSITY OF CALIFORNIA
BERKELEY, CALIFORNIA 94720